

# Continuous Online Adaptation Driven by User Interaction for Medical Image Segmentation

Wentian Xu<sup>1</sup>, Ziyun Liang<sup>1</sup>, Harry Anthony<sup>1</sup>, Yasin Ibrahim<sup>1</sup>, Felix Cohen<sup>1</sup>, Guang Yang<sup>1</sup>, Daniel Whitehouse<sup>2</sup>, David Menon<sup>2</sup>, Virginia Newcombe<sup>2</sup>, and Konstantinos Kamnitsas<sup>1</sup>

<sup>1</sup> Department of Engineering Science, University of Oxford, Oxford, UK

<sup>2</sup> Department of Medicine, University of Cambridge, Cambridge, UK  
wentian.xu@eng.ox.ac.uk

**Abstract.** Interactive segmentation models use real-time user interactions, such as mouse clicks, as extra inputs to dynamically refine the model predictions. After model deployment, user corrections of model predictions could be used to adapt the model to the post-deployment data distribution, countering distribution-shift and enhancing reliability. Motivated by this, we introduce an online adaptation framework that enables an interactive segmentation model to continuously learn from user interaction and improve its performance on new data distributions, as it processes a sequence of test images. We introduce the Gaussian Point Loss function to train the model how to leverage user clicks, along with a two-stage online optimization method that adapts the model using the corrected predictions generated via user interactions. We demonstrate that this simple and therefore practical approach is very effective. Experiments on 5 fundus and 4 brain MRI databases demonstrate that our method outperforms existing approaches under various data distribution shifts, including segmentation of image modalities and pathologies not seen during training. Code and models will be released upon publication.

**Keywords:** Interactive · Segmentation · Continual · Online Adaptation.

## 1 Introduction

Medical image segmentation facilitates disease analysis, diagnosis and treatment. Deep learning methods have driven notable advances in *automated* segmentation but performance can still fall short of expert-level accuracy, particularly when applied to data that differ significantly from the training data. In many workflows, after a model is deployed, clinicians can provide valuable feedback while using it, to guide segmentation results towards expert-level accuracy. **Interactive segmentation** methods leverage this by incorporating user prompts—such as clicks, scribbles or bounding boxes—to inform model predictions.

A common approach for interactive segmentation modeling is to incorporate user prompts as input channels to a Convolutional Network, with DeepIGeoS [19] and Interactive FCNN [15] as representative examples. Other models such as

SAM [6], MedSAM [12], Med-SA [22] encode user-prompts via a Transformer. They have achieved promising performance on natural and medical image benchmarks, demonstrating the benefit of incorporating user prompts.

Standard interactive models, such as the above, optimize parameters on training data without further adaptation to the data processed after model deployment – commonly called the *test data distribution*. This *distribution shift* between test and training data, such as due to acquisition with different scanners, can hinder model performance. Various methods were developed to alleviate this.

For this purpose, a category of interactive methods fine-tune the model *for the specific image* they currently segment [16, 18]. This process is *independent* for each image, restoring the original model parameters before processing the next image. Thus these models do not learn the overall test data distribution.

To account for data shift more holistically and adapt the model to the overall data distribution processed after deployment, **Continuous Adaptation** methods were developed for interactive segmentation. These methods use **Online Learning** [5] to update model parameters after each test image is processed, continuously optimizing model performance as they process the sequence of data. User prompts are exploited to define an optimization objective<sup>3</sup>. Prior work on Continual Online Learning for interactive medical image segmentation is rather limited. An early related method is IA+SA [7], originally developed for natural images, that combines independent image-level adaptation (IA) and image sequence adaptation (SA). A related prior method applied on medical imaging is TSCA, which leverages the teacher-student framework for adaptation [1]. These methods leverage user corrections to optimize the model to the test distribution, using a *sparse* cross-entropy or focal loss defined only on the pixels clicked by the user to update the model. This focuses optimization on the few clicked pixels, neglecting surrounding regions. Hence these methods require additional regularizers to enforce spatial coherence of segmentation, increasing method complexity and hyper-parameters that require tuning.

This study proposes a novel **Online Adaptation for Interactive Medical-image Segmentation (OAIMS)** method that learns from the sequence of data processed after deployment. Guided by the following design principles, the study makes corresponding technical contributions to meet them:

- a) We focus on user interactions via clicks, because they are simple to use for various tasks, such as segmenting tissues with multiple, irregular components. To train a model leverage user clicks effectively, we design the Gaussian Point Loss (GPL) that enforces coherent, correct segmentation of regions around clicks.
- b) Adaptation of interactive models should bolster both the ability to segment and to react after user clicks to correct errors. We designed a two-stage procedure for this: Stage-1 optimizes ability to segment with one localization click; Stage-2 optimizes use of multiple correction clicks. Importantly, we leverage segmentations corrected via user interactions as supervision to learn the new distribution.
- c) We strive for simplicity, as adaptation must be reliable on varying new distri-

<sup>3</sup> Continuous Adaptation in this context optimizes for the test distribution, thus it does not aim to tackle Catastrophic Forgetting of training data as Continual Learning [20].

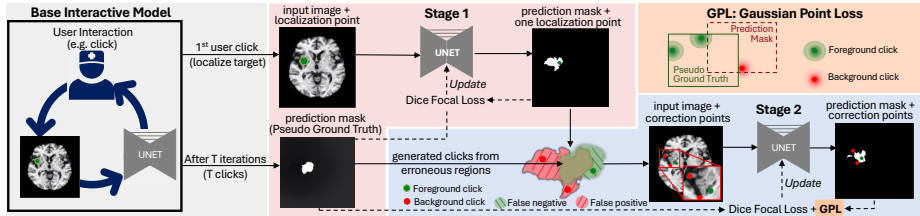


**Fig. 1.** Overview of proposed method. Stage 1: Fine-tune with one localization point as input on final Predicted mask. Stage 2: Fine-tune with multiple correction points and enhance the model’s ability to utilize clicks.

butions in clinical workflows, without oversight by technical experts. We demonstrate this no-frills method outperforms prior approaches on distribution shifts across 5 fundus and 4 brain MRI databases with varying modalities and diseases.

## 2 Methods

The overview of our method is shown in Fig. 1. *To enhance the segmentation performance*, the model is fine-tuned with a pseudo ground truth. This pseudo ground truth is the prediction mask of the **base interactive model** given  $T$  user clicks. In **stage 1**, the model is fine-tuned with only a single localization click as input. In **stage 2**, the output is fine-tuned with additional generated pseudo points as inputs. *To improve the model’s ability to utilize clicks under distribution shift*, a **Gaussian Point Loss (GPL)** is proposed.

We below describe our method for binary segmentation but it can be extended to multi-class settings, as demonstrated in the Experiments section.

### 2.1 Interactive Model

We define the interactive model as  $f(I, C, \theta)$ , where  $I$  is the input image,  $C$  is the set of user-provided clicks, and  $\theta$  represents the model parameters. The user sets  $C$  to the foreground or background class when clicking. During training, the model is trained to predict given  $C$ . During online adaptation, we receive a sequence of images,  $I_1, I_2, \dots, I_n$ . For each image, at each iteration  $t$ , a new click  $c_t$  based on the prediction  $f(I_n, C_{t-1}, \theta)$  is added to the click set  $C_t = C_{t-1} \cup \{c_t\}$ , until it reaches  $C_T$  after  $T$  iterations. The final prediction for an image  $I_n$  is given by  $P_{nT} = f(I_n, C_T, \theta)$ . We then apply the softmax and argmax functions to obtain the final binary segmentation mask,  $P_{n\_final}$ , for image  $I_n$ . For simplicity, we omit the index  $n$  in the subsequent representations.

### 2.2 Online Adaptation Strategy

When adapting interactive segmentation models to a new distribution, it is important to strengthen both their ability to segment and to leverage user clicks

for correcting errors. To improve its segmentation ability, since the final predictions  $f(I, C_T, \theta)$  are made by the base interactive model with the user’s click information, they should implicitly contain the information from the entire click set  $C_T$ . Therefore, we set these final predicted masks as pseudo ground truth labels to guide the adaptation process.

However, enhancing the model’s segmentation capability alone is not enough; improving the ability to leverage user clicks is also important when adapting to new data distributions. Upon receiving a user click, the model should correct the corresponding pixel and the surrounding area correctly based on the click’s class (foreground or background) and the surrounding image structure. However, with data distribution shifts, changes in image structure require relearning the relationship between the corrected area and the surrounding image structure.

Therefore, we introduce **Gaussian Point Loss** (GPL) to ensure the model effectively utilizes user clicks to correct both the corresponding target pixel and its surrounding area to its class label (foreground or background). This loss penalizes incorrect predictions in the pixels near the user click that should have the same class as the clicked point (based on the pseudo-ground), and the confidence of the pixels is weighted using a Gaussian distance ( $G$ ).

$$G(u_{i',j'}, \hat{P}_{i,j}) = \begin{cases} \exp\left(\frac{-(i'-i)^2 + |j'-j|^2}{2\sigma^2}\right) & \text{if } |i' - i| \leq 10 \text{ and } |j' - j| \leq 10, \\ 0 & \text{otherwise.} \end{cases}$$

$$L_{GPL} = \frac{\sum_u \sum_{i=0}^H \sum_{j=0}^W G(u_{i',j'}, \hat{P}(i,j)) \cdot I_{u_{i',j'}}(i,j) \cdot \text{CE}(\hat{P}(i,j), P_{\text{final}}(i,j))}{|u| \cdot H \cdot W}$$

Where  $u_{i',j'}$  represents the user’s click at  $(i', j')$ , while  $\hat{P}(i, j)$  and  $P_{\text{final}}(i, j)$  represent pixel  $(i, j)$  in the new prediction and the pseudo ground truth mask respectively.  $I_{u_{i',j'}}(i, j)$  is a binary mask where  $(i, j)$  is set to 1 if the class of  $P_{\text{final}}(i, j)$  (pseudo ground truth) matches the class (foreground or background) of the click  $u_{i',j'}$ , and 0 otherwise, as visualized in the GPL section in Fig. 1.

Our online adaptation strategy consists of two stages to improve the performance for both one click on the target object and multiple correction clicks.

**Stage 1 - Fine-tune with One Localization Click as Input:** In this stage, we enhance the model’s segmentation ability on a new data distribution with a single localization point as input. We fine-tune the model on the pseudo ground truth by updating the model parameters to let the prediction with only one click  $P_1 = f(I, c_1, \theta)$  match the final prediction  $P_T = f(I, C_T, \theta)$  (the pseudo ground truth). This approach ensures strong performance with just one localization click and continuously updates the model across the input image sequence. The areas unaffected by the corrections will remain unchanged in the final prediction  $P_T$ , ensuring that the general segmentation ability is preserved during retraining.

Specifically, after the user provides  $T$  interactions on the image, we apply a **Dice-Focal loss** [11, 13] between the prediction only given the first click  $P_1$

and the final predicted mask,  $P_{\text{final}}$ , which is obtained using all  $T$  clicks, where Dice-Focal Loss is  $L_{DF} = (1-\alpha) \cdot L_D + \alpha \cdot L_F$ .

**Stage 2 - Fine-tune with Multiple Correction Clicks as Input and Optimizing Click Effectiveness via Gaussian Point Loss:** In this stage, we compute the false positive and false negative areas in the model’s output from stage one (with only one click), by comparing it with the final predicted mask  $P_{\text{final}}$ , and generate one click in each of the erroneous regions (connected components). The maximum number of clicks is  $T$ .

These generated clicks are used as inputs to the model, resulting in a new prediction  $\hat{P}$ . We then apply the proposed **Gaussian Point Loss** to teach the model to use clicks to correctly refine the segmentation. To stabilize the learning process, we also apply the Dice Focal loss to preserve the general information. The total loss is  $L_{\text{total}} = L_{DF} + \beta L_{GPL}$ .

In this step, we generate new correction points. If we directly use the points that are used to generate  $P_{\text{final}}$ , the output will be too similar, so that the loss would not be effective. By generating new points, we ensure that the model’s corrections remain diverse and the learning process continues to improve the model’s ability to leverage clicks. This generated process is based on the previous prediction mask with  $T$  clicks, so no additional help from clinicians is needed.

**Details of the Base Interactive Model:** We use the same architecture as ISFCNN [15] for the base interactive model, which receives clicks as additional input channels. During training, we optimize the model using a combination of Dice-Focal loss and Gaussian Point Loss.

To train and perform inference on the base interactive model, we simulate human guidance and develop an automatic point generation process that places points in incorrectly segmented regions. During training, we generate one point in the largest foreground area and then identify the erroneous regions via connected components. Each component is ranked by size, and a random point is generated within each. We then take the first  $N$  points from this queue, where  $N$  is the desired number of clicks. At inference time, the first point is placed randomly in the largest foreground area, and subsequent points are placed randomly in the largest error regions identified by connected components.

### 3 Experiments

**Setup and Databases** We evaluate our method on two types of data: fundus images and brain MRIs. **For fundus images**, we use five databases: 1) **REFUGE2** [4, 14], 800 cases; 2) **G1020** [3], 1020 cases (232 non-visible optic cups removed); 3) **GS1-Drishti** [17], 101 cases; 4) **GAMMA** [21], 100 cases; 5) **PAPILA** [8], 488 cases (ground truth used is from first expert). We perform multi-class segmentation {0: Background, 1: Outer-ring, 2: Cup} and compute metrics on disc/cup. We train the base interactive model using (1), and online adapt our model to (2, 3, 4, 5). **For brain MRI**, we use four databases: (1) **BRATS2023 - Adult Glioma** [2] (1251 tumor cases, split into 1002 train set and 249 test set), (2) **ATLAS v2.0** [10] (655 stroke lesions cases), (3) **TBI** (143

traumatic brain injury cases) a private database collected in our institutions, (4) **WMH** [9] (60 white matter hyperintensity cases). We test our model in 2D slices by selecting the slice with the largest total lesion area per case and merging all lesions labels into one class. We pretrain on the BRATS train split and evaluate on its test split and other datasets.

For all experiments, for training, the base interactive model is trained with up to 10 clicks per image. During online adaptation, a sequence of images are input to the model. Each image is corrected with 10 iterations with the base interactive model (1 click per iteration,  $T = 10$ ), simulating real-world clinical usage. Then, after 10 iterations, we proceed with stage 1 and stage 2 on that image, and the model updates continuously as it processes the sequence of input images. For every sample, a Dice score is calculated at each iteration  $t$ , and the table in the experiment section shows the average Dice score of the image sequence after 1, 5, and 10 iterations. We use Adam with learning rate  $10^{-4}$  for fundus databases and  $5 \cdot 10^{-5}$  for Brain MRI. We set  $\alpha = 0.7$  for Dice-Focal loss and  $\beta = 200$  for GPL. The parameter  $\sigma$  in GPL is set to 3.

We implement IA+SA [7] and TSCA [1] baselines using the same trained base interactive model as our method for fair comparison. We use same learning rate as ours, as this improves their method performance over their default.

**Evaluation on Fundus Databases:** We first evaluate our method on several fundus databases with multi-class segmentation. Tab. 1 shows the average Dice score for both disc and cup segmentation. ISFCNN\* [15] is our base interactive model which is kept frozen during testing. The other three methods continually adapt the base interactive model to the new data distribution: IA+SA [7] and TSCA [1] are previous works, and OAIMS is our online learning strategy.

On G1020 and PAPILA, where the data distribution shift is large, our method outperforms previous methods, and all adaptation approaches outperform the base interactive model. On GS1 and GAMMA, where the data distribution shift is small, our method’s performance remains comparable or better. Notably, our method achieves optimal predictions with just two backpropagations per image, while TSCA requires ten and IA+SA even more.

Moreover, these results show online adaptation methods can effectively handle multi-class segmentation. We also observe that IA+SA and TSCA perform similarly, with TSCA slightly better, aligning with previous studies [1]. Thus, we compare only with TSCA in subsequent experiments for simplicity.

**Adapting to Different Brain MRI Modalities:** In this section, we adapt our model to scenarios with larger data distribution shifts. We evaluate our method on different MRI modalities: the model is trained on BRATS with the Flair modality and then tested on T1, T1c, and T2 scans. As shown in Tab. 2, all the online adaptation methods outperform the base interactive model ISFCNN, with T1 gaining substantial improvement. Among online adaptation methods, OAIMS attains the best results, surpassing TSCA by an average of 11.9%, 9.2%, and 4.6% across the three scores. We also compare with the Medical SAM adapter, where our base model, ISFCNN, excels in handling modality shifts.

**Table 1.** Performance on fundus imaging. Base interactive model is trained on REFUGE. Each image receives 10 clicks. Table shows the average Dice (%). TSCA and OAIMS (ours) results are averaged over three runs. Best marked in bold.

Method	G1020			PAPILA			GS1			GAMMA			
	No. Clicks	1	5	10	1	5	10	1	5	10	1	5	10
ISFCNN* (Disc)		89.4	93.1	95.1	88.3	92.6	94.6	96.6	97.2	97.7	94.4	96.3	97.2
ISFCNN* (Cup)		77.4	83.1	88.0	60.3	70.2	77.1	82.4	90.4	94.1	83.3	89.8	93.3
IA+SA (Disc)		90.5	94.3	96.1	89.4	93.3	95.3	96.8	97.4	98.0	94.7	96.3	97.4
IA+SA (Cup)		77.8	84.5	90.3	61.3	70.5	77.6	83.4	91.5	94.8	84.0	90.2	93.9
TSCA (Disc)		89.9	94.2	96.1	89.6	94.0	96.1	96.9	97.5	98.0	94.6	96.4	<b>97.5</b>
TSCA (Cup)		77.6	85.0	90.7	61.7	72.2	79.0	85.4	92.9	95.5	84.2	90.7	<b>94.1</b>
OAIMS(Ours) (Disc)		<b>93.5</b>	<b>95.9</b>	<b>97.0</b>	<b>94.1</b>	<b>96.1</b>	<b>97.0</b>	<b>97.3</b>	<b>97.7</b>	<b>98.2</b>	<b>95.3</b>	<b>96.5</b>	<b>97.5</b>
OAIMS(Ours) (Cup)		<b>81.9</b>	<b>88.5</b>	<b>92.2</b>	<b>73.0</b>	<b>80.0</b>	<b>85.8</b>	<b>89.5</b>	<b>94.1</b>	<b>95.7</b>	<b>85.9</b>	<b>91.4</b>	<b>94.1</b>

**Table 2.** Performance on different brain MRI modalities, best marked in bold.

Method	BRATS T1			BRATS T1c			BRATS T2			
	No. Clicks	1	5	10	1	5	10	1	5	10
ISFCNN*		20.3	34.1	45.3	45.7	61.1	70.9	73.7	81.1	85.0
Medsam Adapter		16.3	21.2	21.4	38.3	41.6	42.3	72.6	74.7	75.2
TSCA		35.1	58.3	69.9	52.1	68.7	78.2	76.9	84.0	87.6
OAIMS(Ours)		<b>59.6</b>	<b>67.1</b>	<b>72.2</b>	<b>65.9</b>	<b>77.7</b>	<b>83.1</b>	<b>83.3</b>	<b>88.3</b>	<b>90.8</b>

We also test our model on the same-modality (Flair) test set instead of cross-modalities. ISFCNN\* achieves 96.4%. Its high performance demonstrates the effectiveness of our base interactive model. Our model achieves 96.3%, showing comparable performance without degradation on similar data distributions.

We also test our method’s performance when we use a smaller number of iterations (fewer user clicks) during online adaptation. We test the model on the BRATS T1 and T1c using only three user clicks. For T1, the Dice scores (in %) for ISFCNN\*, TSCA, and ours are 28.0, 46.5, and 57.5, respectively. For T1c, these scores are 54.9, 59.8, and 71.8, respectively. These findings demonstrate that our approach consistently outperforms TSCA with fewer clicks and remains effective even when the base interactive model’s prediction mask is of poor quality.

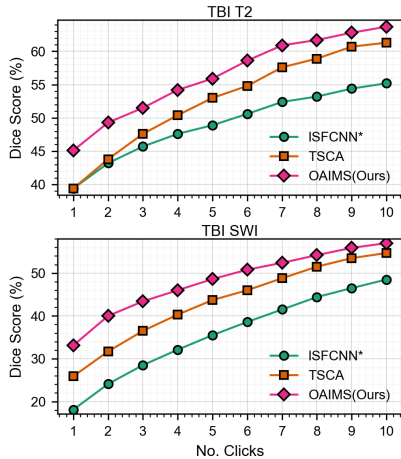
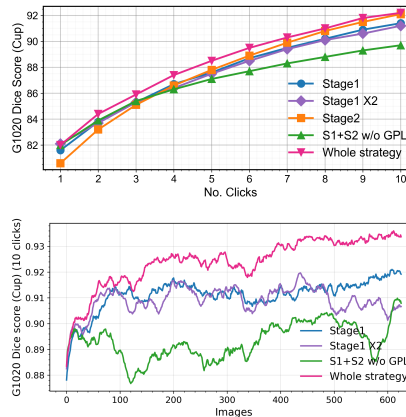
**Adapting to Different Brain Pathologies:** In addition, we tested our model on various brain pathologies - including TBI, WMH, and ATLAS - where the model is trained on either BRATS FLAIR or BRATS FLAIR/T1/T1c together as shown in Tab. 3. Even in these challenging settings, online adaptation methods significantly boost performance, with our approach outperforming previous methods on almost all tasks, especially notable on the challenging ATLAS. For TBI, our model achieves comparable results to the TSCA after ten clicks, but we achieve higher Dice with fewer clicks and require fewer backpropagation steps.

Finally, in cases involving modality and pathology shifts as shown in Fig. 2, our method maintains trends observed in previous experiments, demonstrating effective adaptation even under significant distribution shifts.

**Ablation Study:** We conduct an ablation study on G1020 (cup), shown in Fig. 3. The top panel compares four ablation variants across different numbers

**Table 3.** Performance on different brain pathologies, best marked in bold.

Method	Trained on BRATS(Flair)						Trained on BRATS(Flair,T1,T1c)					
	TBI Flair			WMH Flair			TBI T1			ATLAS T1		
No. Clicks	1	5	10	1	5	10	1	5	10	1	5	10
ISFCNN*	46.2	57.7	63.4	45.1	57.9	65.3	42.0	49.3	55.3	40.6	46.8	52.1
TSCA	48.5	63.8	72.4	52.3	<b>65.8</b>	71.6	44.4	55.8	63.9	43.4	55.7	64.0
OAIMS(Ours)	<b>53.7</b>	<b>68.0</b>	<b>72.5</b>	<b>53.9</b>	64.6	<b>72.4</b>	<b>47.7</b>	<b>61.1</b>	<b>68.0</b>	<b>62.7</b>	<b>77.0</b>	<b>81.8</b>

**Fig. 2.** Adapting to different brain pathologies and MRI modalities. Pre-trained on BRATS(Flair/T1/T1c)**Fig. 3.** Ablation study of proposed components. Dice score for different number of user clicks (top) and images seen during adaptation (bottom).

of clicks: *Stage1* applies only the first-stage of our method; *Stage1*  $\times 2$  applies two backpropagation rounds in stage 1 (matching computational cost of the two-stage approach); *Stage2* only employs the second-stage of our method; and *S1+S2 w/o GPL* combines both stages but omits the GPL loss. Overall our full approach (whole strategy) performs best. Dropping stage 2 leads to performance drop with more clicks, while omitting stage 1 yields poor results at lower clicks.

In the bottom panel of Fig. 3, we set aside 20% of the G1020 dataset as a separate test set and evaluate the model on this set after processing each incoming image. We compare the full strategy with ablation variants that do not include the GPL. As more images are processed, our full approach gradually outperforms the ablated variants. Approaches that omit GPL or stage 2 either improve slowly, fluctuate, or degrade over time.

## 4 Conclusion

This study proposed an online adaptation method for interactive segmentation that enhances the model’s utilization of user clicks and performance on new data



distributions, leveraging the Gaussian Point Loss and a two-stage optimization approach. Experiments demonstrate promising performance on diverse distribution shifts, including unseen MRI modalities and pathologies. These findings highlight the potential of adaptive interactive segmentation to facilitate clinical and research applications.

**Acknowledgments.** ZL is supported by scholarship provided by the EPSRC Doctoral Training Partnerships programme [EP/W524311/1]. HA is supported by a scholarship via the EPSRC Doctoral Training Partnerships programme [EP/W524311/1, EP/T517811/1]. YI is supported by the EPSRC Centre for Doctoral Training in Health Data Science (EP/S02428X/1). VN, NIHR Rosetrees Trust Advanced Fellowship, NIHR302544, is funded in partnership by the NIHR and Rosetrees Trust. The views expressed are those of the authors and not necessarily those of the NIHR, Rosetrees Trust or the Department of Health and Social Care.

## References

1. Atanyan, B., Khachatryan, L., Navasardyan, S., Wei, Y., Shi, H.: Continuous adaptation for interactive segmentation using teacher-student architecture. In: Proceedings of the IEEE/CVF Winter Conference on Applications of Computer Vision. pp. 789–799 (2024)
2. Baid, U., Ghodasara, S., Mohan, S., Bilello, M., Calabrese, E., Colak, E., Farahani, K., Kalpathy-Cramer, J., Kitamura, F.C., Pati, S., et al.: The rsna-asnr-miccai brats 2021 benchmark on brain tumor segmentation and radiogenomic classification. arXiv preprint arXiv:2107.02314 (2021)
3. Bajwa, M.N., Singh, G.A.P., Neumeier, W., Malik, M.I., Dengel, A., Ahmed, S.: G1020: A benchmark retinal fundus image dataset for computer-aided glaucoma detection. In: 2020 International Joint Conference on Neural Networks (IJCNN). pp. 1–7. IEEE (2020)
4. Fang, H., Li, F., Wu, J., Fu, H., Sun, X., Son, J., Yu, S., Zhang, M., Yuan, C., Bian, C., et al.: Refuge2 challenge: A treasure trove for multi-dimension analysis and evaluation in glaucoma screening. arXiv preprint arXiv:2202.08994 (2022)
5. Hoi, S.C., Sahoo, D., Lu, J., Zhao, P.: Online learning: A comprehensive survey. *Neurocomputing* **459**, 249–289 (2021)
6. Kirillov, A., Mintun, E., Ravi, N., Mao, H., Rolland, C., Gustafson, L., Xiao, T., Whitehead, S., Berg, A.C., Lo, W.Y., et al.: Segment anything. In: Proceedings of the IEEE/CVF International Conference on Computer Vision. pp. 4015–4026 (2023)
7. Kontogianni, T., Gygli, M., Uijlings, J., Ferrari, V.: Continuous adaptation for interactive object segmentation by learning from corrections. In: Computer Vision—ECCV 2020: 16th European Conference, Glasgow, UK, August 23–28, 2020, Proceedings, Part XVI 16. pp. 579–596. Springer (2020)
8. Kovalyk, O., Morales-Sánchez, J., Verdú-Monedero, R., Sellés-Navarro, I., Palazón-Cabanes, A., Sancho-Gómez, J.L.: Papila: Dataset with fundus images and clinical data of both eyes of the same patient for glaucoma assessment. *Scientific Data* **9**(1), 291 (2022)

9. Kuijff, H., Biesbroek, M., de Bresser, J., Heinen, R., Chen, C., van der Flier, W., Barkhof, Viergever, M., Biessels, G.J.: Data of the White Matter Hyperintensity (WMH) Segmentation Challenge (2022). <https://doi.org/10.34894/AECRSD>, <https://doi.org/10.34894/AECRSD>
10. Liew, S.L., Lo, B.P., Donnelly, M.R., Zavaliangos-Petropulu, A., Jeong, J.N., Barisano, G., Hutton, A., Simon, J.P., Juliano, J.M., Suri, A., et al.: A large, curated, open-source stroke neuroimaging dataset to improve lesion segmentation algorithms. *Scientific data* **9**(1), 320 (2022)
11. Lin, T.Y., Goyal, P., Girshick, R., He, K., Dollár, P.: Focal loss for dense object detection. In: *Proceedings of the IEEE international conference on computer vision*. pp. 2980–2988 (2017)
12. Ma, J., He, Y., Li, F., Han, L., You, C., Wang, B.: Segment anything in medical images. *Nature Communications* **15**(1), 654 (2024)
13. Milletari, F., Navab, N., Ahmadi, S.A.: V-net: Fully convolutional neural networks for volumetric medical image segmentation. In: *2016 fourth international conference on 3D vision (3DV)*. pp. 565–571. Ieee (2016)
14. Orlando, J.I., Fu, H., Breda, J.B., Van Keer, K., Bathula, D.R., Diaz-Pinto, A., Fang, R., Heng, P.A., Kim, J., Lee, J., et al.: Refuge challenge: A unified framework for evaluating automated methods for glaucoma assessment from fundus photographs. *Medical image analysis* **59**, 101570 (2020)
15. Sakinis, T., Milletari, F., Roth, H., Korfiatis, P., Kostandy, P., Philbrick, K., Akkus, Z., Xu, Z., Xu, D., Erickson, B.J.: Interactive segmentation of medical images through fully convolutional neural networks. *arXiv preprint arXiv:1903.08205* (2019)
16. Sambaturu, B., Gupta, A., Jawahar, C., Arora, C.: Efficient and generic interactive segmentation framework to correct mispredictions during clinical evaluation of medical images. In: *Medical Image Computing and Computer Assisted Intervention–MICCAI 2021: 24th International Conference, Strasbourg, France, September 27–October 1, 2021, Proceedings, Part II 24*. pp. 625–635. Springer (2021)
17. Sivaswamy, J., Krishnadas, S., Joshi, G.D., Jain, M., Tabish, A.U.S.: Drishti-gs: Retinal image dataset for optic nerve head (onh) segmentation. In: *2014 IEEE 11th international symposium on biomedical imaging (ISBI)*. pp. 53–56. IEEE (2014)
18. Wang, G., Li, W., Zuluaga, M.A., Pratt, R., Patel, P.A., Aertsen, M., Doel, T., David, A.L., Deprest, J., Ourselin, S., et al.: Interactive medical image segmentation using deep learning with image-specific fine tuning. *IEEE transactions on medical imaging* **37**(7), 1562–1573 (2018)
19. Wang, G., Zuluaga, M.A., Li, W., Pratt, R., Patel, P.A., Aertsen, M., Doel, T., David, A.L., Deprest, J., Ourselin, S., et al.: Deepigeos: a deep interactive geodesic framework for medical image segmentation. *IEEE transactions on pattern analysis and machine intelligence* **41**(7), 1559–1572 (2018)
20. Wang, L., Zhang, X., Su, H., Zhu, J.: A comprehensive survey of continual learning: Theory, method and application. *IEEE Transactions on Pattern Analysis and Machine Intelligence* (2024)
21. Wu, J., Fang, H., Li, F., Fu, H., Lin, F., Li, J., Huang, Y., Yu, Q., Song, S., Xu, X., et al.: Gamma challenge: glaucoma grading from multi-modality images. *Medical Image Analysis* **90**, 102938 (2023)
22. Wu, J., Ji, W., Liu, Y., Fu, H., Xu, M., Xu, Y., Jin, Y.: Medical sam adapter: Adapting segment anything model for medical image segmentation. *arXiv preprint arXiv:2304.12620* (2023)